Proc. Natl. Acad. Sci. USA
Vol. 87, pp. 8017–8021, October 1990
Neurobiology

Gangliosides normalize distorted single-cell intracellular free Ca^{2+} dynamics after toxic doses of glutamate in cerebellar granule cells

(neurotoxicity/fura-2 imaging/calcium homeostasis/double labeling fluorescence microscopy)

GABRIEL A. DE ERAUSQUIN, HARI MANEV, ALESSANDRO GUIDOTTI, ERMINIO COSTA, AND GARY BROOKER

Fidia–Georgetown Institute for the Neurosciences and Department of Biochemistry and Molecular Biology, Georgetown University, Washington, DC 20007

Contributed by Erminio Costa, August 6, 1990

ABSTRACT **Glutamate-induced delayed neurotoxicity after abusive and paroxismal activation of its receptors has been proposed to depend upon a sustained increase in intracellular free Ca^{2+} ($[Ca^{2+}]_i$). To elucidate the temporal and causal relationship between glutamate-induced changes in $[Ca^{2+}]_i$ and neuronal death, we simultaneously studied the dynamics of $[Ca^{2+}]_i$ changes in single neurons with the acetoxymethyl ester of fura-2 and the cell viability by imaging the nuclear penetration of propidium iodide. The main difference between toxic (50 μM) and nontoxic (5 μM) doses of glutamate is the lack of regulation in $[Ca^{2+}]_i$ 20 min after glutamate is removed. This protracted rise in $[Ca^{2+}]_i$ in a single cell is correlated with ($r = 0.87$, $P < 0.01$, Spearman's test), and consequently predictive of, the time of appearance of neuronal death, as measured by propidium iodide fluorescence. In addition, the glutamate receptor antagonists dibenzocycloheptenimine (MK-801) and 3,3-(2-carboxypiperazine-4-yl)propyl 1-phosphate reduce the acute increase of $[Ca^{2+}]_i$ induced by glutamate but fail to revert the protracted increase of $[Ca^{2+}]_i$, elicited by toxic doses of glutamate. In contrast, the ganglioside GM_1 and the semisynthetic lysoGM$_1$ with *N*-acetylsphingosine (LIGA-4) and lysoGM$_1$ with *N*-dichloroacetylsphingosine (LIGA-20) failed to change the immediate rise of $[Ca^{2+}]_i$ elicited by glutamate but prevented the protracted increase in $[Ca^{2+}]_i$ after toxic doses of glutamate. Voltage-dependent Ca^{2+} channel blockers (nifedipine, etc.) did not change the initial or protracted responses to glutamate.**

Glutamate receptor abusive stimulation triggers a disruption of intracellular calcium homeostasis (1–4) and the amplification of pathogenic processes associated with cell injury during ischemia and post-ischemic neuronal death (5–7). In fact, a dose of glutamate able to induce neuronal death in primary cultures of hippocampal pyramidal cells results in an increase in intracellular free Ca^{2+} ($[Ca^{2+}]_i$), which persists far beyond the removal of the toxin from the medium (2). Furthermore, the delay in the recovery of resting $[Ca^{2+}]_i$ levels parallels the extent of neuronal death 24 hr later (2). In addition, it has been reported that when cultures of hippocampal neurons are exposed to Mg^{2+}-free glycine-supplemented medium, there are large spontaneous oscillations in $[Ca^{2+}]_i$ that parallel further development of cell death (6). Furthermore, these fluctuations are dependent on the presence of glycine and are blocked by pretreatment with *N*-methyl-D-aspartate (NMDA) antagonists (6). Again, this pharmacology is shared by cell death induced by the same conditions (6).

In cerebellar granule neurons in culture, glutamate also induces delayed cell death which is triggered by the NMDA receptor and also amplified by $[Ca^{2+}]_i$ (1, 4). This proposal is supported by evidence showing that extracellular free Ca^{2+} is critical during the post-glutamate period for the cell death to develop and that $^{45}Ca^{2+}$ uptake is increased after a toxic, but not after a nontoxic, exposure to glutamate (4, 7, 8). Since delayed toxicity is triggered by processes that need to be amplified by Ca^{2+} to induce cell death, another approach for therapeutical drug targeting can be directed to act on the Ca^{2+} amplification events without altering receptor responsiveness to glutamate that is vital to normal cell function (7). We refer to this strategy as receptor abuse-dependent antagonism, and we have shown (4, 7) that either natural gangliosides or their semisynthetic derivatives are able to fill its requirements. In fact, pretreatment of cerebellar granule neurons with these drugs completely prevents glutamate-induced delayed neuronal death, as well as protracted $^{45}Ca^{2+}$ uptake, without modifying glutamate-induced channel opening features (7, 8).

However, in spite of the fact that agents that modify the glutamate excitotoxicity have parallel effects on the $[Ca^{2+}]_i$ homeostasis destabilization, there is no clear evidence related either to the temporal or to the causal relationship between the two phenomena in individual cells. Therefore, we developed a microscopic imaging technique to simultaneously evaluate in the same cell, the dynamics of $[Ca^{2+}]_i$ changes by using a fluorescent probe, the acetoxymethyl ester of fura-2 (fura-2 AM) (9), and the neuronal viability by simultaneously imaging permeation to the nuclear dye propidium iodide, a marker of viability (1). We have found that the main difference between toxic and nontoxic doses of glutamate is the existence of a protracted increase in $[Ca^{2+}]_i$ after glutamate removal and that this protracted rise in $[Ca^{2+}]_i$ in a single given cell is correlated with, and consequently predictive of, the time of appearance of neuronal death, as measured by propidium iodide fluorescence. In addition we found that ganglioside GM_1, and the semisynthetic gangliosides lysoGM$_1$ with *N*-acetylsphingosine (LIGA-4) and lysoGM$_1$ with *N*-dichloroacetylsphingosine (LIGA-20), which are all able to prevent the development of the glutamate neurotoxicity by way of a receptor abuse-dependent antagonism mechanism, also prevented the $[Ca^{2+}]_i$ increase that persists after glutamate withdrawal and the propidium iodide uptake.

MATERIALS AND METHODS

Primary Cultures of Cerebellar Granule Cells. Our *in vitro* model has been described in detail elsewhere (10). Briefly, we used 7- to 8-day-old primary cultures of rat cerebellar granule cells prepared from 8-day-old Sprague–Dawley rats (Zivic-Miller, Pittsburgh). Neurons were grown in 35-mm culture dishes containing 25-mm glass coverslips (Fischer Scientific no. 1) coated with poly(L-lysine). Glial proliferation was prevented by adding cytosine arabinonucleoside (10 μM, final concentration) 24 hr after plating. Immunocytochemical

The publication costs of this article were defrayed in part by page charge payment. This article must therefore be hereby marked "*advertisement*" in accordance with 18 U.S.C. §1734 solely to indicate this fact.

Abbreviations: $[Ca^{2+}]_i$, intracellular free Ca^{2+}; NMDA, *N*-methyl-D-aspartate; PKC, protein kinase C; AM, acetoxymethyl ester.

studies of these primary cultures of cerebellar granule cells showed that they contain >95% neurons and <5% glia or other contaminating cells (10). Because of the distinct morphological differences between neurons and glia, Ca^{2+} imaging data were derived only from neurons.

Fluorescence Imaging. The cells grown on glass coverslips were loaded with 5 μM fura-2 AM for 30 min in Locke's buffer (154 mM NaCl/5.6 mM KCl/3.6 mM $NaHCO_3$/2.3 mM $CaCl_2$/1.2 mM $MgCl_2$/5.6 mM glucose/5 mM Hepes, pH 7.4) at 37°C and then mounted in a 35-mm holder that created a chamber with the coverslip on the bottom (11). After loading with fura-2 and before the beginning of the experiments, the cells were given 5–10 min to allow fura-2 deesterification and equilibration between the bound and free forms. In experiments with propidium iodide, 0.7 μM propidium iodide was added to the perfusion fluid and was present at all times during the experiment. The cells were imaged using an Attofluor digital fluorescence microscopy system (Atto Instruments, Potomac, MD). The system consisted of a Zeiss ICM-405 inverted epifluorescence microscope with all-quartz optics. A 100-W mercury burner served as the source for excitation. Both fura-2 and propidium iodide were excited at the wavelength pair of 334 nm and 390 nm by using 10-nm bandpass interference filters, which were alternately selected by the computer-controlled excitation and shutter control unit. The $[Ca^{2+}]_i$ was measured by the ratio of fura-2 fluorescence excited by 334 nm to that excited by 390 nm and calibrated according to external standards (12, 13). A Zeiss dichromatic beam splitter (FT 395) was used to separate the excitation beam from emission image. Emission of both dyes was monitored with an intensified charge-coupled devise camera whose sensitivity was set for each wavelength and then switched to that sensitivity by the computer just before each wavelength of excitation was selected. A 510-nm long-pass emission filter was used to select fluorescence emission above 500 nm when only fura-2 was imaged. For simultaneous fura-2 and propidium iodide imaging, a combination emission filter set was used for fura-2 imaging. This emission combination prevents propidium iodide emission interference with the fura-2 image. To measure the red propidium iodide fluorescence free of interference from the fura-2 emission, the emission filter was switched to a red emission wavelength filter that excluded emission below 640 nm. The video signals were digitized to 8-bit resolution (256 shades of gray, 512 × 512 pixels per frame); in real time and in most cases, five images were captured and averaged during a 320-msec shutter opening of the excitation source. In addition to automatic capture and disk storage of the 334-nm and 390-nm image pairs and/or ratioed images, the system also continuously calculated and graphically displayed the mean intensity of a variable-size pixel box area located on one of the cells in the field of view. The outline of the box is seen on the images. For fura-2 images, the instrument was operated in the calibrated mode, in which background subtraction and correlation to Ca^{2+} standards were performed in real time, such that Ca^{2+} concentration within the selected box area was displayed in graphical form versus time (for equation, see ref. 12). For propidium iodide, images were taken every 5 min at 334 nm with background subtraction. For statistical calculations of propidium iodide data, the average pixel intensity (at 334-nm excitation) of a 96-pixel box area was considered. A data file of the pixel intensities for both dyes and Ca^{2+} concentration was saved by the computer.

Drug Treatments. Drugs, dissolved in Locke's solution, were perfused over the cells at 1 ml/min with a peristaltic pump while the cells were being imaged. $MgCl_2$ was routinely omitted from the solution during the exposure to glutamate (5–20 min, 22°C). The volume in the dish was 500 μl. For ganglioside treatment, solutions were incubated 1 hr at 37°C before using them, then cell monolayers were preincubated either (*i*) with GM_1 (100 μM; Fidia, Abano Terme, Italy) alone for 90 min and then 30 min with GM_1 plus fura-2 or (*ii*) with fura-2 AM alone for 15 min and then 15 min with LIGA-4 (7 μM; Fidia) plus fura-2 AM or LIGA-20 (3.5 μM; Fidia) plus fura-2 AM. Thereafter, the cultures were washed three times with Locke's solution and then set in the perfusion system. Images presented are of a field per figure. Experiments were performed at room temperature (≈22°C).

Statistics. For averaging of temporal curves the *z* transformation was used (mean subtraction and then division by the SD). For the correlation between $[Ca^{2+}]_i$ and viability, the Spearman rank correlation test was performed. Finally, a one-way analysis of variance was used for dose–response curves and a two-way analysis of variance for the effects of additional treatments. All the statistical calculations were done using the corresponding routines of STATGRAF (version 2.1; Statistical Graphic Systems, Rockville, MD).

RESULTS

Glutamate-Induced Ca^{2+} Rise Is Dose- and Time-Dependent. The glutamate-induced rise in $[Ca^{2+}]_i$ during perfusion with glutamate in Mg^{2+}-free buffer is time- and dose-dependent as shown in Figs. 1 and 2. Perfusion with Mg^{2+}-free Locke's solution alone did not change basal $[Ca^{2+}]_i$ ($[Ca^{2+}]_i$ = 37 ± 5 nM and see below). However, in Mg^{2+}-containing buffer, either 5 μM glutamate ($[Ca^{2+}]_i$ = 52 ± 2 nM) or 50 μM glutamate ($[Ca^{2+}]_i$ = 64 ± 6 nM) was unable to induce consistent rises in $[Ca^{2+}]_i$, while the response to 500 μM glutamate ($[Ca^{2+}]_i$ = 110 ± 25 nM) was markedly reduced under these conditions. Furthermore, perfusion with 1 μM dibenzocycloheptenimine (MK-801) had no effect on basal $[Ca^{2+}]_i$ and when started 1 min before application of glutamate suppressed all changes in $[Ca^{2+}]_i$ in response to concentrations of glutamate up to 500 μM.

Toxic Concentrations of Glutamate Induce Protracted Destabilization of $[Ca^{2+}]_i$. In these cultures, a short exposure to 50 μM, but not to 5 μM glutamate in Mg^{2+}-free buffer, followed by the removal of glutamate, results in neuronal

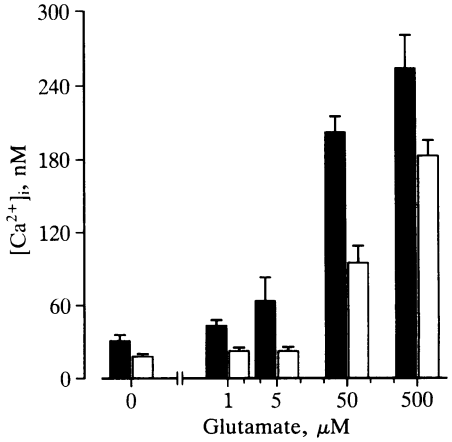

FIG. 1. $[Ca^{2+}]_i$ at 5 min (open bars) and 20 min (solid bars) continuous exposure to various doses of glutamate. Cells were prelabeled with fura-2 AM and then stimulated with either Mg^{2+}-free Locke's solution alone (bars 0) or with the same solution containing 1, 5, 50, or 500 μM glutamate (as indicated by labels of bars) at room temperature (≈22°C) for either 5 or 20 min. Each bar represents the mean ± SEM of a field of cells (n = 6–9 cells). Since these responses show priming by previous exposure to glutamate (i.e., if the same cell is repeatedly exposed to glutamate the rise in $[Ca^{2+}]_i$ is bigger the second time than it would be in a naive cell after the same dose), the data presented were obtained by exposing each culture to a different and unique dose.

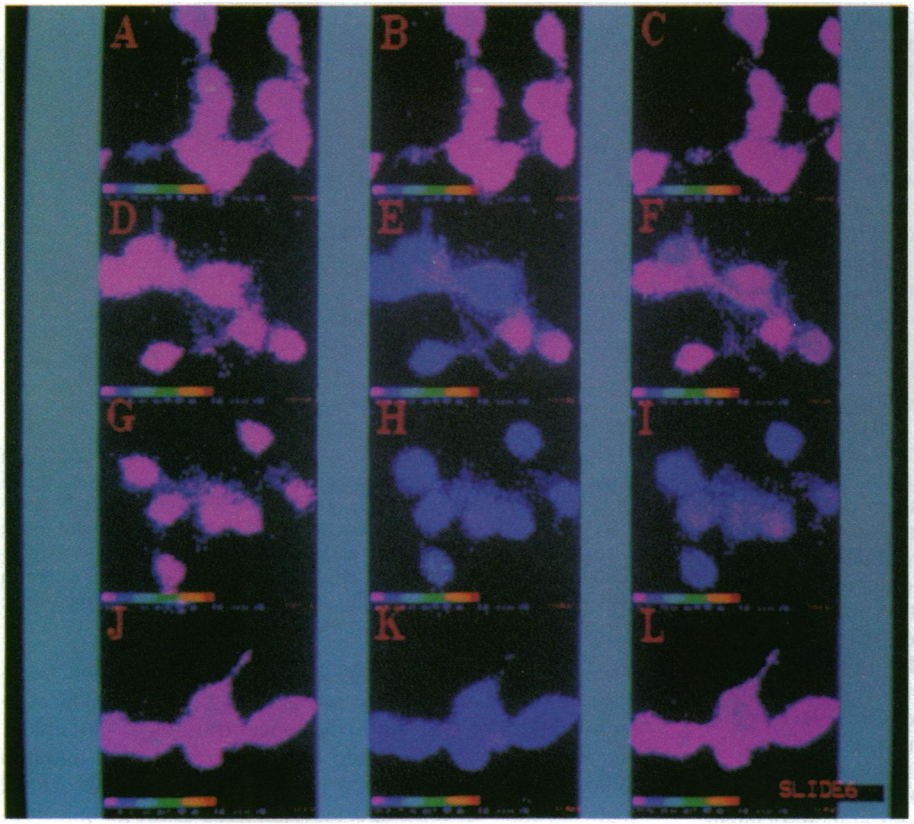

FIG. 2. Toxic vs. nontoxic glutamate induced changes in $[Ca^{2+}]_i$ during and after glutamate exposure in cerebellar granule cells. Time sequence images of fura-2-calibrated $[Ca^{2+}]_i$ 334/390-nm fluorescence. (*A*, *D*, *G*, and *J*) Basal (perfusion with Locke's buffer with Mg^{2+}). (*B*, *E*, *H*, and *K*) A 20-min perfusion with one of the following solutions. (*B*) Locke's without Mg^{2+}. (*E*) Glutamate (5 μM). (*H* and *K*) Glutamate (50 μM). (*C*, *F*, *I*, and *L*) Fifteen minutes after removal of glutamate and continuous perfusion with Locke's buffer with Mg^{2+}. (*J–L*) Cells were preincubated 2 hr before applying glutamate in buffer with 100 μM GM_1. All cultures were loaded 30 min with fura-2 AM as described. Color scale at bottom of each picture depicts pixel intensity of the ratio image multiplied by 50. Basal background fluorescence was <5% of the peak fluorescence and was subtracted from each image. $[Ca^{2+}]_i$ in the cells is detailed in the text.

death that begins to become evident after 2–3 hr and fully develops after 24 hr (1, 4). Here, we compared the effect of perfusing 5 μM and 50 μM glutamate for 20 min on the $[Ca^{2+}]_i$ in single cells, followed by a 15-min period of washing in Mg^{2+}-containing Locke's buffer. Fig. 2 *A–C* shows that the granule cell $[Ca^{2+}]_i$ does not change spontaneously during the time span of a typical experiment, if the perfusion contains only Mg^{2+}-free buffer. In turn, 5 μM glutamate (Fig. 2 *D–F*), a dose that is not ultimately toxic to the cells, causes an initial increase in $[Ca^{2+}]_i$ that returns to basal within 15 min after removal of glutamate and washing with Mg^{2+}-containing buffer. The pattern of the response extracted from the average of five normalized curves (from five experiments, each curve representing a single cell probed by the box in real time) is depicted in Fig. 3. This rise in $[Ca^{2+}]_i$ induced by 5 μM glutamate remained as long as the perfusion with glutamate was continued. However, when the culture was exposed to 50 μM glutamate for the same period of time, the dynamic changes in $[Ca^{2+}]_i$ were protracted such that the $[Ca^{2+}]_i$ 15 min after removing glutamate from the bath remained high, as shown in Fig. 2 *G–I*. The averaged normalized trace is shown in Fig. 3. The average $[Ca^{2+}]_i$ for six to nine cells was determined by reference to our calibration. It was 37 ± 5 nM for basal, 85 ± 37 nM for 5 μM glutamate, and 175 ± 39 nM for 50 μM glutamate. The glutamate-induced changes in $[Ca^{2+}]_i$ are dependent upon Mg^{2+} concentration. If Mg^{2+} is raised to 1.2 mM, concentrations of glutamate >5 mM are required to produce similar time course alterations in $[Ca^{2+}]_i$ homeostasis. However, in the presence of 1.2 mM Mg^{2+}, glutamate destabilization of $[Ca^{2+}]_i$ with 50 μM glutamate is still observed under depolarizing conditions (25 mM KCl).

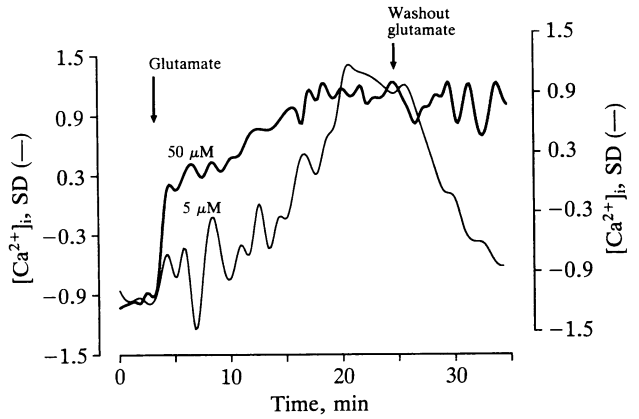

FIG. 3. Time course of 5 μM (thin line) or 50 μM (thick line) glutamate effect on $[Ca^{2+}]_i$. Cells were prelabeled 30 min with fura-2 AM and then challenged with either 5 μM or 50 μM glutamate. Each curve is a normalized average of calibrated $[Ca^{2+}]_i$ of five experiments—i.e., the curves were averaged after subtracting the mean and dividing by its standard deviation (SD). Note that the $[Ca^{2+}]_i$ is then expressed as SDs of the mean.

Sustained Elevation in $[Ca^{2+}]_i$ After a Toxic Concentration of Glutamate Does Not Involve Glutamate Receptors. In cells treated with 50 μM glutamate for 20 min, $[Ca^{2+}]_i$ remains elevated 15 min after the replacement of glutamate by buffer with Mg^{2+} (120 ± 23 nM compared to a basal $[Ca^{2+}]_i$ of 37 ± 3.5 nM). A perfusion with the NMDA receptor antagonist 3,3-(2-carboxypiperazine-4-yl)propyl 1-phosphate (CPP, 40 μM) failed to reduce the increase of $[Ca^{2+}]_i$ after glutamate withdrawal ($[Ca^{2+}]_i$ = 170 ± 25 nM). Furthermore, 1 μM MK-801 did not cause a statistically significant decline in the $[Ca^{2+}]_i$ enhanced by a previous exposure to glutamate ($[Ca^{2+}]_i$ = 90 ± 47 nM). The quisqualate receptor antagonist 6-cyano-7-nitroquinoxaline-2,3-dione (CNQX, 1 μM) also failed to restore the basal level ($[Ca^{2+}]_i$ = 118 ± 36 nM). Moreover, blockers of voltage-dependent Ca^{2+} channels such as NiCl (1 mM) or nifedipine (10 μM) also failed to revert the sustained $[Ca^{2+}]_i$ elevation ($[Ca^{2+}]_i$ = 182 ± 59 nM and

$[Ca^{2+}]_i$ = 133 ± 47 nM, respectively). Yet, the protracted increase in $[Ca^{2+}]_i$ is partly dependent on the extracellular-free Ca^{2+} since removal of the cation from the bath by chelation with 5 mM EGTA completely reverted the process in about 50% of the cells evaluated.

Post-Glutamate $[Ca^{2+}]_i$ Predicts the Time Course of Viability Loss in Individual Cells. In this series of experiments, we directly evaluated the relationship between fura-2 fluorescence to measure $[Ca^{2+}]_i$ and propidium iodide fluorescence to measure cell viability. Propidium iodide is a charged polar compound that only penetrates damaged cell membranes and interacts with nuclear DNA yielding a bright red fluorescent complex (14). The paralleled dynamic changes of $[Ca^{2+}]_i$ and of propidium iodide neuronal influx after a toxic dose of glutamate are shown in Fig. 4. It is worth noting that in spite of the marked ongoing changes in $[Ca^{2+}]_i$ during and up to 30 min after the toxic pulse of glutamate the cells are completely viable. However, Fig. 4 shows that, starting about 2 hr after removal of the toxic concentration of glutamate, most of the cells show a further and larger increase in $[Ca^{2+}]_i$, which precedes by about 10 min the first appearance of propidium iodide fluorescence, indicating loss of viability. Strikingly, the time sequence of cells showing propidium iodide staining is correlated with the degree of alteration in $[Ca^{2+}]_i$ after removing toxic doses of glutamate, so that the latter is predictive of the former, and this correlation is statistically very significant according to the Spearman test ($r = 0.88$; $P < 0.005$). Moreover, in the same cells the $[Ca^{2+}]_i$ level either in basal conditions (i.e., before glutamate exposure) ($r = 0.45$; $P > 0.10$) or in steady-state conditions (at 20-min glutamate exposure) ($r = 0.67$; $P < 0.05$) did not correlate with the time of viability loss as well as post-glutamate levels did, showing that destabilization of $[Ca^{2+}]_i$ homeostasis in the post-glutamate period, and not basal $[Ca^{2+}]_i$, is a critical index of cell death.

Gangliosides Normalize Distorted Single Cell $[Ca^{2+}]_i$ Dynamics After a Toxic Concentration of Glutamate. Since gangliosides protect against glutamate neurotoxicity (1, 4, 7), we studied their effect on $[Ca^{2+}]_i$ dynamics during and after a toxic concentration of glutamate. Fig. 5 shows that either the naturally occurring ganglioside GM_1 (100 μM, 2-hr pretreatment) or the semisynthetic derivatives LIGA-4 (7 μM, 15 min) and LIGA-20 (3.5 μM, 15 min) completely prevented the protracted elevation of $[Ca^{2+}]_i$ after the toxic pulse. In other experiments not shown here, a pretreatment with natural and semisynthetic gangliosides prevented glutamate toxicity in the presence of 1.2 mM Mg^{2+} either with 5 mM glutamate in absence of depolarization or 50 μM glutamate under depolarizing conditions (25 mM KCl). Ca^{2+} images for GM_1-pretreated cells are shown in Fig. 2 *J–L*, showing the protective effect of GM_1 on toxic concentrations of glutamate. Gangliosides also prevented the appearance of propidium iodide fluorescence up to 3 hr after glutamate withdrawal (data not shown). It is important that none of the gangliosides tested prevented the initial rise in $[Ca^{2+}]_i$ during exposure to toxic doses of glutamate, suggesting that they fail to change receptor stimulation by glutamate.

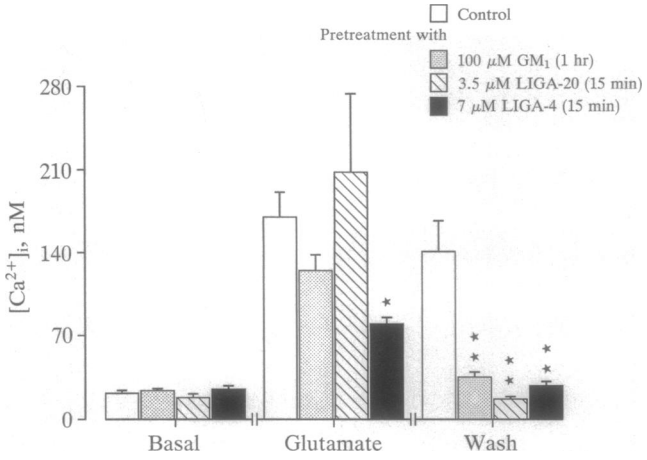

FIG. 5. Effect of gangliosides GM_1, LIGA-4, and LIGA-20 on single-cell $[Ca^{2+}]_i$ dynamics during and after perfusion with 50 μM glutamate. Each bar represents the mean ± SEM of three fields (n = 6–9 cells per field). Bars: glutamate, $[Ca^{2+}]_i$ after a 20-min glutamate exposure; wash, $[Ca^{2+}]_i$ after a 15-min continuous wash with Mg^{2+}-containing Locke's buffer; basal, $[Ca^{2+}]_i$ after a 20-min exposure to Mg^{2+}-containing Locke's buffer. ★, $P < 0.05$ compared to control; ★★, $P < 0.01$ compared to control.

DISCUSSION

In primary cultures of cerebellar granule cells, the delayed neurotoxicity induced by glutamate is dependent upon persistent stimulation of NMDA-sensitive glutamate receptor for appropriate time periods. Such a protracted stimulation leads to a destabilization of $[Ca^{2+}]_i$ homeostasis expressed as a sustained increase in $[Ca^{2+}]_i$ after removal of glutamate. The present data are consistent with our previous results with the same neuronal cultures using $^{45}Ca^{2+}$ uptake and viability studies (4, 8) and with the results of others (2, 5, 6) using fura-2 fluoromicroscopy in hippocampal cultured neurons.

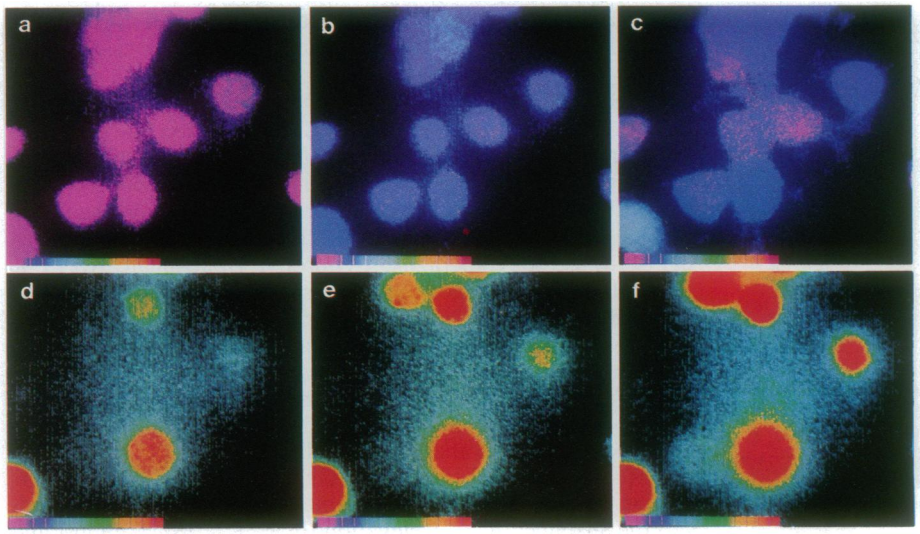

FIG. 4. Simultaneous imaging of changes in $[Ca^{2+}]_i$ and cell viability after 50 μM glutamate. Cells were loaded with fura-2 AM as described and then exposed for 20 min to glutamate, and afterwards the glutamate was washed out by perfusion in Locke's solution containing Mg^{2+}. Propidium iodide (0.7 μM) was present in the perfusion solution at all times. Time course of $[Ca^{2+}]_i$ is shown in *a–c*. (*a*) Basal. (*b*) After 20 min of continuous glutamate. (*c*) Fifteen minutes after the removal of glutamate. (*d–f*) Time course of propidium iodide fluorescence in the same cells 2 hr, 2 hr and 10 min, and 2 hr and 20 min, respectively, after removal of glutamate. Propidium iodide fluorescence was not seen at any time in control cells or in cells treated either with the nontoxic concentrations of glutamate or with toxic concentrations of glutamate in ganglioside pretreatment conditions.

Moreover, they are consistent with the evidence that removal of extracellular free Ca^{2+} is partly effective in restoring basal levels of $[Ca^{2+}]_i$ after withdrawal of neurotoxic doses of glutamate (4).

An important technical feature of the present study is the ability to simultaneously determine the $[Ca^{2+}]_i$ and propidium iodide uptake that allows us to correlate the $[Ca^{2+}]_i$ response and delayed death of individual neurons after glutamate exposure. Because of the extremely high sensitivity of the image-intensified detection system used, we were able to obtain a precise propidium iodide uptake profile after glutamate, which allows us to infer that the neurodegenerative changes and the processes that mediate them are well underway within 2 hr after exposing the cells to excitotoxic glutamate concentrations. Furthermore, a protracted increase in $[Ca^{2+}]_i$ after toxic doses of glutamate is related to the time course of the development of degenerative changes in the same neuron, as detected by nuclear staining with propidium iodide. Since there is a quantitative correlation between them, one can infer that the former is probably causally linked to the latter.

It is usually assumed that $[Ca^{2+}]_i$ increase after glutamate is sustained by a continuing influx of Ca^{2+} (2, 4, 7). Yet, the nature of the alteration in Ca^{2+} homeostasis remains to be clarified. Intracellular Ca^{2+} homeostasis depends upon influx, intracellular redistribution, and efflux of Ca^{2+}. Influx can occur through either receptor-gated or voltage-gated Ca^{2+} channels. Intracellular ionic redistribution is known to be regulated by (*i*) the endoplasmic reticulum uptake, (*ii*) the release of Ca^{2+} from endoplasmic reticulum stores mainly linked to inositol phospholipid production, (*iii*) a mitochondrial Ca^{2+} pump, and (*iv*) the buffering capacity of cytosolic proteins. Ca^{2+} efflux from the neurons occurs by the active outward transport of Ca^{2+} through the Ca^{2+}-ATPase and by the activity of the Na^+–Ca^{2+} exchanger (15).

The present study indicates that protracted increase in $[Ca^{2+}]_i$ after glutamate is not related to sustained NMDA receptor activation nor with opening of voltage-dependent Ca^{2+} channels, because their respective blockers, in doses known to be active on granule cells, failed to regulate $[Ca^{2+}]_i$ after removing glutamate. Accordingly, we have reported (4) that these drugs do not protect against delayed neurotoxicity when applied to granule cells in the postglutamate period. Although we have not directly measured Ca^{2+} release from intracellular stores, the dependence of excitotoxicity on extracellular Ca^{2+} during a critical period of 30 min after glutamate withdrawal seems to rule out the participation of intracellular Ca^{2+} stores as a cause of neuronal death. In addition, Ca^{2+} release from intracellular stores has been postulated to evoke wide oscillations in $[Ca^{2+}]_i$, a feature completely absent in the present experiments with granule cells. Therefore, the evidence presented indicates, albeit indirectly, that intracellular Ca^{2+} release might not be involved in causing the persistent increase in $[Ca^{2+}]_i$ levels after a toxic dose of glutamate. The remaining possibilities are that either the extrusion process or intracellular uptake might be altered in such a way as to reduce the homeostatic capacity of the system. An alternative pathway that can explain the $[Ca^{2+}]_i$ increase in neurons exposed to toxic doses of glutamate might be the Na^+–Ca^{2+} exchanger. During the postglutamate period there is an excessive activation and membrane translocation of the cytosolic protein kinase C (PKC). The activity of this enzyme appears to be also necessary for the development of glutamate excitotoxicity because the prevention of PKC translocation by gangliosides or its downregulation by prolonged treatment with phorbol esters prevents glutamate neurotoxicity (4, 8). Moreover, both procedures prevent the delayed increase in $^{45}Ca^{2+}$ uptake (4, 8). Since naturally occurring the ganglioside (GM_1) or their semisynthetic derivatives (LIGA-4 and LIGA-20) prevent the sustained increase in $[Ca^{2+}]_i$ elicited by neurotoxic doses of glutamate, the hypothesis that PKC-protracted activation and translocation are a necessary intermediate step leading to the delayed loss of $[Ca^{2+}]_i$ homeostasis appears to be upheld (1, 4, 8). Interestingly, sphingosine, which also inhibits PKC, prevents the appearance of the sustained Ca^{2+} gradients generated in the apical dendrites of isolated hippocampal neurons by glutamate applications (3). Therefore, the PKC-mediated phosphorylation of one or more membrane processes participating in $[Ca^{2+}]_i$ homeostasis can be implicated in the development of glutamate neurotoxicity. The target of PKC activity is still a matter for speculation, but undoubtedly the Ca^{2+}-ATPase and the Na^+–Ca^{2+} exchanger are appealing possibilities. Whether ganglioside pretreatment reduces glutamate neurotoxicity by preventing PKC translocation remains to be determined.

We thank Drs. R. Llinas and J. Connor for their helpful comments. This work was supported by National Institutes of Health Grants HL 28940 and NS 28130.

1. Favaron, M., Manev, H., Alho, H., Bertolino, M., Ferret, B., Guidotti, A. & Costa, E. (1988) *Proc. Natl. Acad. Sci. USA* **85,** 7351–7355.
2. Ogura, A., Miyamoto, M. & Kudo, Y. (1988) *Exp. Brain Res.* **73,** 447–458.
3. Connor, J. A., Wadman, W. J., Hockberger, P. E. & Wong, R. K. (1988) *Science* **240,** 649–653.
4. Manev, H., Favaron, M., Guidotti, A. & Costa, E. (1989) *Mol. Pharmacol.* **36,** 106–112.
5. Choi, D. (1988) *Neuron* **1,** 623–634.
6. Abele, A. E., Scholz, K. P., Scholz, W. K. & Miller, R. J. (1990) *Neuron* **2,** 413–419.
7. Manev, H., Favaron, M., Vicini, S., Guidotti, A. & Costa, E. (1990) *J. Pharmacol. Exp. Ther.* **252,** 419–427.
8. Favaron, M., Manev, H., Siman, R., Bertolino, M., Szekely, A. M., de Erausquin, G. A., Guidotti, A. & Costa, E. (1990) *Proc. Natl. Acad. Sci. USA* **87,** 1983–1987.
9. Tsien, R. Y., Rink, T. J. & Poenie, M. (1985) *Cell Calcium* **6,** 145–147.
10. Vaccarino, F. M., Alho, A., Santi, M. R. & Guidotti, A. (1987) *J. Neurosci.* **7,** 65–76.
11. Ince, C., van Dissel, J. T. & Diesselhoff, M. M. C. (1985) *Pflügers Arch.* **403,** 240–244.
12. Connor, J. A. (1986) *Proc. Natl. Acad. Sci. USA* **83,** 6179–6183.
13. Brooker, G., Seki, T., Croll, D. & Wallestedt, C. (1990) *Proc. Natl. Acad. Sci. USA* **87,** 2813–2817.
14. Jones, K. H. & Senft, J. A. (1985) *J. Histochem. Cytochem.* **33,** 77–79.
15. Carafoli, E. (1987) *Annu. Rev. Neurosci.* **56,** 395–433.